MTL TR 89-26

AD

OXIDATION AND HOT CORROSION OF SOME ADVANCED SUPERALLOYS AT 1300°F TO 2000°F (740°C TO 1093°C)

MILTON LEVY and ROBERT M. HUIE
U.S. ARMY MATERIALS TECHNOLOGY LABORATORY
METALS RESEARCH BRANCH

FRED PETTIT
UNIVERSITY OF PITTSBURGH

April 1989

US ARMY
LABORATORY COMMAND
MATERIALS TECHNOLOGY LABORATORY

U.S. ARMY MATERIALS TECHNOLOGY LABORATORY
Watertown, Massachusetts 02172-0001

The findings in this report are not to be construed as an official Department of the Army position, unless so designated by other authorized documents.

Mention of any trade names or manufacturers in this report shall not be construed as advertising nor as an official indorsement or approval of such products or companies by the United States Government.

DISPOSITION INSTRUCTIONS

Destroy this report when it is no longer needed.
Do not return it to the originator.

UNCLASSIFIED

SECURITY CLASSIFICATION OF THIS PAGE *(When Data Entered)*

REPORT DOCUMENTATION PAGE		READ INSTRUCTIONS BEFORE COMPLETING FORM
1. REPORT NUMBER MTL TR 89-26	2. GOVT ACCESSION NO.	3. RECIPIENT'S CATALOG NUMBER
4. TITLE *(and Subtitle)* OXIDATION AND HOT CORROSION OF SOME ADVANCED SUPERALLOYS AT 1300°F TO 2000°F (704°C TO 1093°C)		5. TYPE OF REPORT & PERIOD COVERED Final Report 6. PERFORMING ORG. REPORT NUMBER
7. AUTHOR(s) Milton Levy, Robert M. Huie, and Fred Pettit*		8. CONTRACT OR GRANT NUMBER(s)
9. PERFORMING ORGANIZATION NAME AND ADDRESS U.S. Army Materials Technology Laboratory Watertown, Massachusetts 02172-0001 SLCMT-EMM		10. PROGRAM ELEMENT, PROJECT, TASK AREA & WORK UNIT NUMBERS D/A Project: 1L162105.AH84
11. CONTROLLING OFFICE NAME AND ADDRESS U.S. Army Laboratory Command 2800 Powder Mill Road Adelphi, Maryland 20783-1145		12. REPORT DATE April 1989 13. NUMBER OF PAGES 20
14. MONITORING AGENCY NAME & ADDRESS *(if different from Controlling Office)*		15. SECURITY CLASS. *(of this report)* Unclassified 15a. DECLASSIFICATION/DOWNGRADING SCHEDULE

16. DISTRIBUTION STATEMENT *(of this Report)*

Approved for public release; distribution unlimited.

17. DISTRIBUTION STATEMENT *(of the abstract entered in Block 20, if different from Report)*

18. SUPPLEMENTARY NOTES

*University of Pittsburgh, Pittsburgh, PA 15161

19. KEY WORDS *(Continue on reverse side if necessary and identify by block number)*

Superalloys
Nickel-base superalloys
Oxidation resistance
Corrosion
Sulfidation

20. ABSTRACT *(Continue on reverse side if necessary and identify by block number)*

(SEE REVERSE SIDE)

DD FORM 1 JAN 73 1473 EDITION OF 1 NOV 65 IS OBSOLETE

UNCLASSIFIED

SECURITY CLASSIFICATION OF THIS PAGE *(When Data Entered)*

Block No. 20

ABSTRACT

The cyclic oxidation resistance and the hot corrosion resistance of three single crystal nickel-base superalloys and DS MAR M 200 are compared. The comparison is made by using burner rig oxidation tests at 2000°F (1093°C), and tube furnace oxidation and hot corrosion tests at 2000°F (1093°C), 1650°F (900°C), and 1300°F (704°C). The rig tests and the tube furnace tests produce similar results with the single crystal alloys being more oxidation resistant than DS MAR M 200. A significant difference between the hot corrosion resistance of these alloys was not observed. All four alloys were extremely susceptible to hot corrosion induced by a liquid deposit. Keywords: Sodium Sulfates, (HW)

CONTENTS

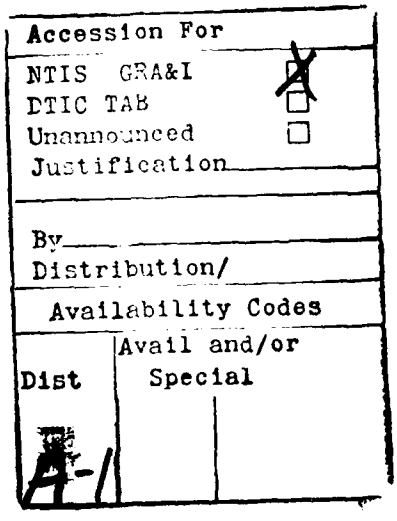

INTRODUCTION

Superalloy solidification procedures are now available whereby single crystal gas turbine blades can be fabricated. Superalloys with such structures have certain mechanical properties that are superior to conventionally cast and directionally solidified alloys.[1] Since the single crystal alloys do not require alloying elements to provide grain boundary strengthening, their compositions are different and somewhat less complicated than their polycrystalline counterparts. In a previous paper,[2] the oxidation resistances of several single crystal superalloys in air at 2000°F (1093°C) were compared to a polycrystalline alloy, DS MAR M 200,* under both isothermal and cyclic conditions. The oxidation resistances of all the single crystal alloys were superior to the polycrystalline alloy. A significant difference between the oxidation of the different single crystal alloys was not observed.

In this previous investigation, the cyclic oxidation tests were performed by using a tube furnace in which the specimens were cycled to room temperature once every one-half hour of exposure at 2000°F (1093°C). Another method of oxidation testing is to use a dynamic burner rig.[3,4] Burner rig testing often utilizes high gas velocities (200 to 300 m/sec) and, while not reproducing the exact conditions in a gas turbine, it does simulate more closely such conditions than does the tube furnace oxidation test. One of the objectives of this report is to compare the oxidation behavior of the single crystal alloys and DS MAR M 200 by using dynamic burner rig testing at 2000°F (1093°C), as well as tube furnace cyclic oxidation testing at 2000°F (1093°C) and 1650°F (900°C).

For some gas turbine operating conditions, deposits may accumulate upon the surfaces of turbine hardware. The compositions of such deposits depend upon the operating conditions (e.g., fuel impurities, air contaminants, and temperatures). Very often, the deposits are sulfates containing sodium and calcium. Such deposits can significantly affect the degradation of superalloys at temperatures of 1300°F (704°C) and above. Another objective of this report is to compare the Na_2SO_4-induced hot corrosion of the single crystal superalloys to DS MAR M 200 by using tube furnace tests at 1650°F (900°C) and 1300°F (704°C).

EXPERIMENTAL

Table 1 presents the nominal compositions of the alloys used in this study. To protect the proprietary rights of the various alloy manufacturers that supplied material, the compositions are simply identified by a letter rather than by their commercial name. A state-of-the-art directionally solidified alloy (DS MAR M 200 with hafnium) has been included for comparison purposes.

*Registered trade name.

1. GELL, M., DUHL, D. N., and GIAMEI, A. F. *Superalloys 1980.* TIEN, J. K., WLODEK, S. T., MORROW, III, H., GELL, M., MAURER, G., ed., American Society for Metals, Metals Park, Ohio, 1980, p. 205.
2. LEVY, M., FARRELL P., and PETTIT, F. *Oxidation of Some Advanced Single-Crystal Nickel-Base Superalloys in Air at 2000°F (1093°C).* Corrosion, v. 42, no. 12, 1986, p. 708.
3. DOERING, H. V., and BERGMAN, P. A. Mat. Res. Stand, v. 9, 1969, p. 35.
4. DILS, R. R., and FOLLENSBEE, P. S. Corrosion, v. 33, 1977, p. 385.

Table 1. NOMINAL COMPOSITIONS OF ALLOYS (WEIGHT PERCENT)

Designation	Ni	Cr	Co	Mo	W	Ta	Ti	Al	Cb	Hf
Alloy A	bal	10	5		4	12	1.5	5		
Alloy B	bal	7.5	4	0.5	7.5	6	0.9	5.5		0.1
Alloy C	bal	8	5	0.5	8	6	1	5.5		
DS MAR M 200	bal	8.75	10		12		2	5	1	3

All of the alloys were received as 1.3-cm to 1.6-cm (0.5-in. to 0.63-in.) diameter rods. From these rods, specimen discs 1.3 cm (0.5 in.) in diameter and 3-mm (0.118 in.) thick were fabricated. These discs were polished through 600 grit SiC paper, scrubbed with hot soapy water, and rinsed with acetone before being used in the cyclic oxidation and hot corrosion tests. The burner rig specimens were also machined from these rods. Their bases were cylindrically shaped, 1.3 cm (0.5 in.) in diameter, and 2.4 cm (0.95 in.) long. The remainder of these specimens were 8 cm (3.15 in.) long and wedge shaped. The leading edge of the wedge had the curvature of the original cylinder, and an average length of 3 cm (1.2 in.). The trailing edge had an average length 0.3 cm (0.12 in.) and the center was about 1.3 cm (0.5 in.) from the center of the leading edge. The surfaces of the burner rig specimens were not polished after final machining to a 90 RMS finish.

The laboratory tube furnace apparatus that was used for the cyclic oxidation and cyclic hot corrosion tests has been described previously.[2] It consists of an electrically heated vertical tube furnace with the bottom sealed to inhibit convective flow. A suspension chain and an electrically motorized arm are used to move the specimens cyclically into and out of the hot zone of the furnace through the top end. The specimens remain in the hot zone for 30 minutes and then in the cool zone (just outside the furnace) for 5 minutes, where they cool to 212°F (100°C). The cyclic oxidation tests were performed at 2000°F (1093°C) and 1650°F (900°C) in air. The cyclic not corrosion tests employed temperatures of 1650°F (900°C) and 1300°F (704°C) in air. The specimens usually were examined after every 20 hours of exposure; however, when the attack was not substantial, exposure and observation intervals of 150 hours were used. The specimens were examined using a low power microscope and weighed. In the case of the hot corrosion tests, the specimens were coated with about 1 mg/cm^2 of Na_2SO_4. This deposit was applied by heating specimens to 250°F (121°C) and spraying them with an aqueous mist saturated with Na_2SO_4. The specimens were coated with the deposit at the beginning of the test. They were washed in hot water at each observation period prior to weighing. A new deposit was applied just prior to the next exposure.

The burner rig was used only to assess the oxidation behavior of the alloys at 2000°F (1093°C). This type of rig has been described in the literature.[3,4] It consists of a combustor with the specimens placed on a rotating platform in front of the nozzle from which the hot gases emerged. The specimens were exposed at test temperature for 12 minutes and then exposed to forced air cooling for 4 minutes. The fuel was JP5. The specimen platform held eight erosion bars and it was rotated at 120 rpm. The specimen temperature was measured by using a two-color pyrometer (Ircon Modline).

All of the alloys subjected to oxidation or hot corrosion conditions in each of the test methods were sectioned and mounted using standard metallographic techniques. When etching was required, AG21 (50-cm^3 lactic acid, 30-cm^3 HNO_3, and 2-cm^3 HF) was used. All specimens were examined by optical metallography and scanning electron microscopy (SEM).

RESULTS AND DISCUSSION

Characterization of the As-Received Specimens

The four cast alloys identified in Table 1 were solution heat treated at 2350°F to 2400°F (1288°C to 1315°C) for 2 to 4 hours and then air cooled. The resulting microstructures have been described in previous papers.[1,2,5] All of the single crystal alloys contained a fine (0.2 μ - 0.5 μ) dispersion of γ' particles in a γ matrix. In addition, these alloys contained a much larger globular shaped γ' (enriched in Ta and W). The former γ' was formed upon cooling below the solvus of the γ-phase, whereas the latter evidently developed during freezing of the liquid, and is often referred to as eutectic γ'. The MAR M 200 alloy contained fine γ', eutectic γ' at grain boundaries, and carbides all in a matrix of γ-phase.

Cyclic Oxidation

The cyclic oxidation was performed at 2000°F and 1650°F (1093°C and 900°C). In the case of the testing at 2000°F (1093°C), weight change data are presented in Figure 1 for both burner rig and tube furnace tests. If weight loss is used as a means of comparing the alloys in these tests, both tests give the same ranking of the alloys. In particular, MAR M 200 has undergone more degradation than any of the single crystal alloys. For both tests, all of the single crystal alloys require at least twice the exposure time as MAR M 200 to have the same weight loss. In the case of the tube furnace test, there is not a significant difference in weight loss between any of the single crystal alloys. The burner rig data show smaller losses for Alloy A than for Alloys B or C. The ranking of the oxidation resistances of the single crystal alloys must be done with care since the differences in weight losses are not large, and all the oxidation products may not spall from the specimen surfaces. Optical metallographic and scanning electron microscope observations of the exposed specimens also must be considered in making these comparisons.

In Figures 2 through 5, photographs are presented to compare the microstructural features that developed during the degradation of MAR M 200 and the single crystal alloys in the tube furnace test and in the burner rig. Photographs to show the degradation of MAR M 200 after 250 hours in the cyclic oxidation furnace are presented in Figure 2. A thick external scale has been formed and internal oxidation of the aluminum to form a discontinuous subscale is evident. The etched specimen in this figure exhibits an aluminum-depleted zone below a thick external oxide scale and a subscale zone. The degradation microstructure of MAR M 200 after 80 hours in the burner rig test at 2000°F (1093°C) is presented in Figure 3. The microstructural features developed in this alloy are considered to be identical in both tests. The microstructural features that developed in the single crystal alloys during exposure in the cyclic tube furnace and in the burner rig are presented in Figures 4 and 5, respectively. Zones depleted of γ' have been developed in both tests with localized regions having thick scales of oxide. In the zones depleted of γ', a phase having a platelet shape has been formed. This phase does not develop in MAR M 200. It has been determined to contain nickel, tungsten, tantalum, and molybdenum, and to be susceptible to preferential oxidation. With the exception of the platelet phase, the microstructural features of the MAR M 200 are very similar to those of the single crystal alloys. As shown in a previous paper,[2] both MAR M 200 and all of the single crystal alloys are Al_2O_3 formers when oxidized isothermally with different amounts of transient oxidation occurring before these

5. GIGGINS, C. S., and PETTIT, F. S. J. Electrochem. Soc., v. 118, 1971, p. 1782.

Al_2O_3 scales develop continuity. Hence, in cyclic oxidation tests such as those used in the present investigation, the similarity between the degraded microstructures is to be expected.

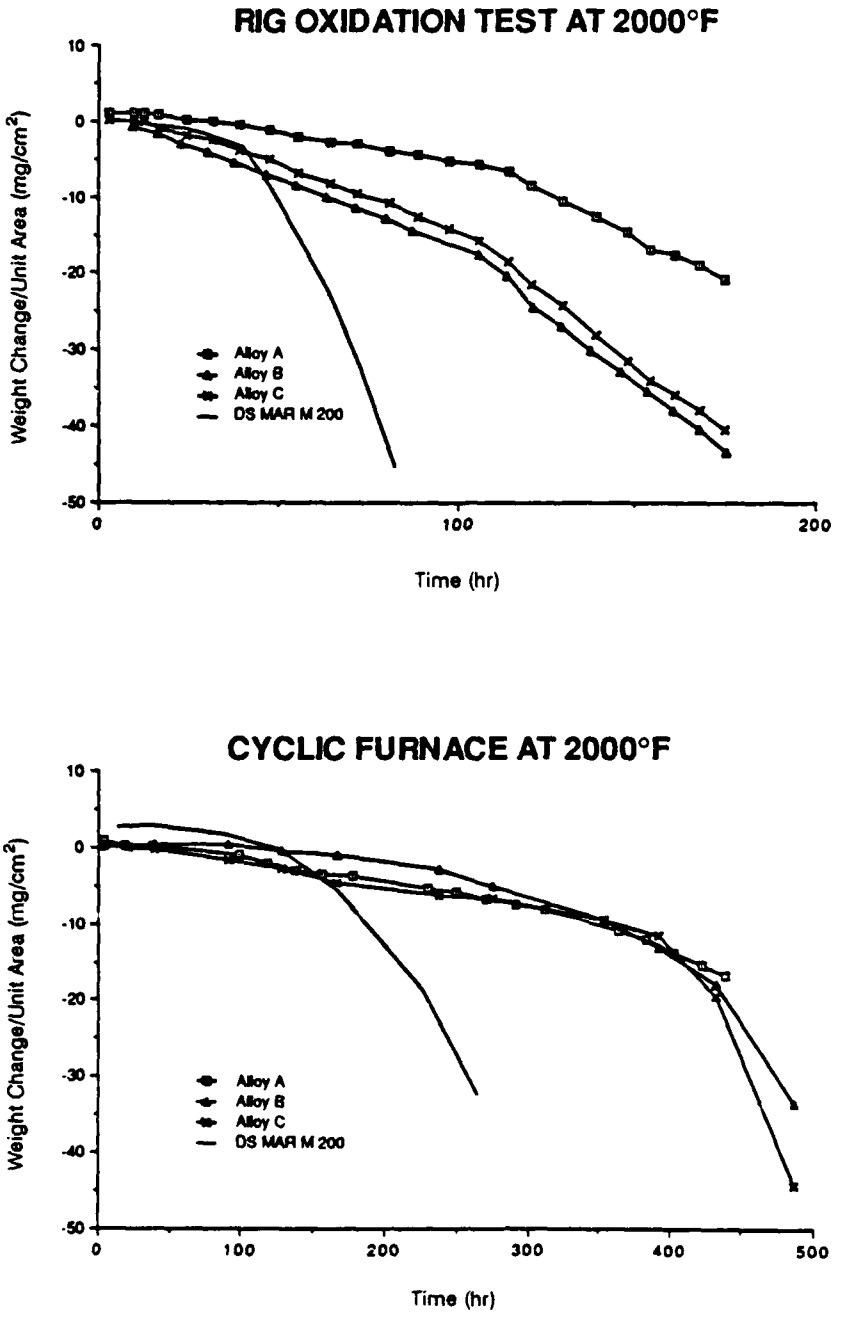

Figure 1. Weight change data for both burner rig and cyclic furnace tests at 2000°F.

Figure 2. Typical microstructure that developed during cyclic oxidation of MAR M 200 in the tube furnace test at 2000°F (1093°C).

Figure 3. Typical microstructure that developed during cyclic oxidation of MAR M 200 in the burner rig at 2000°F (1093°C).

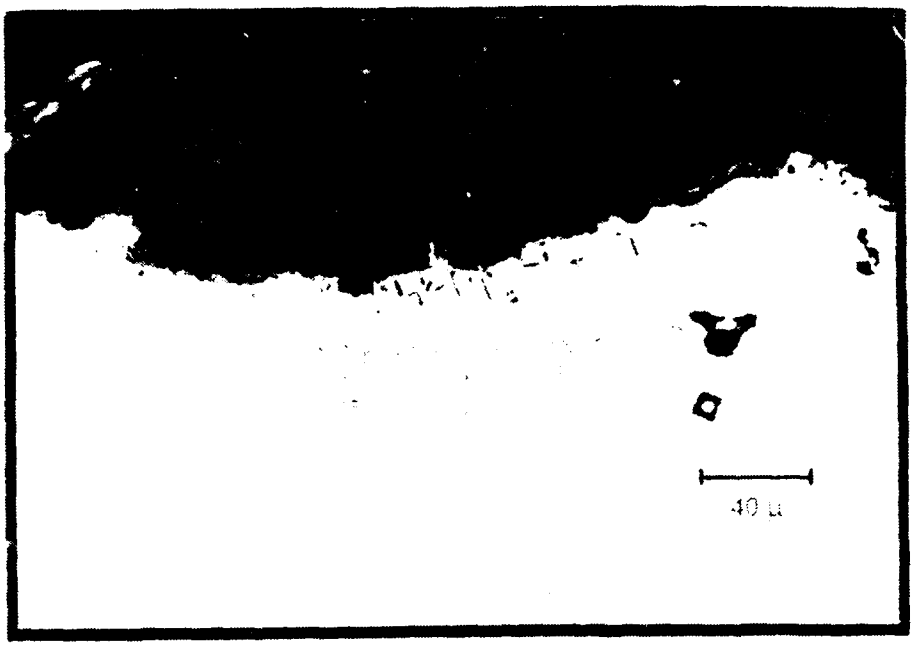

Figure 4. Typical microstructure that developed during cyclic oxidation of single crystal superalloys in the tube furnace at 2000°F (1093°C), (Alloy B).

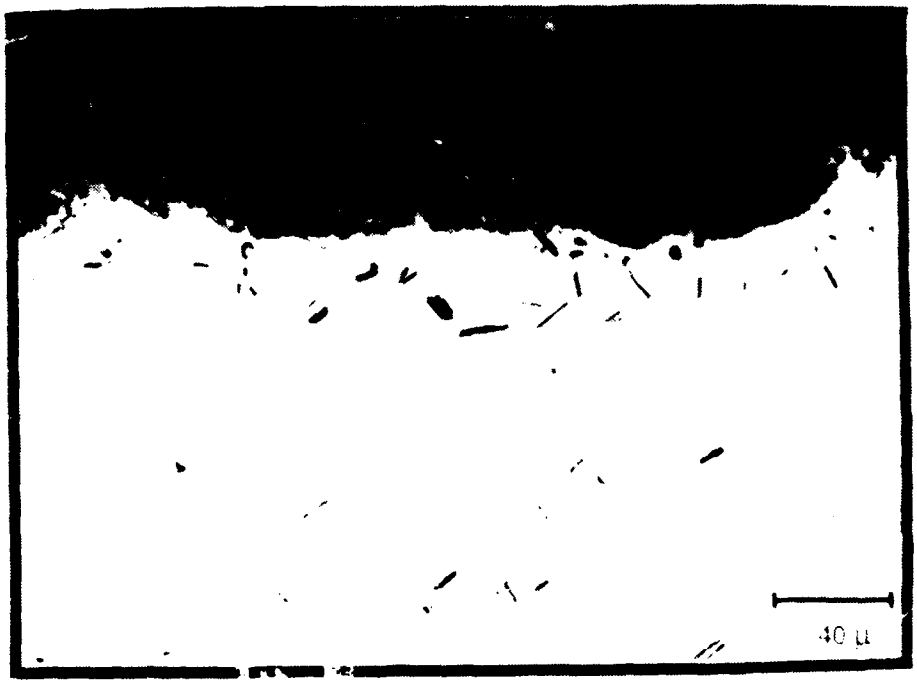

Figure 5. Typical microstructure that developed during cyclic oxidation of single crystal superalloys at 1650°F (900°C).

The weight change data for the cyclic oxidation of the alloys at 1650°F (900°C) are presented in Figure 6. The weight change data are weight gains rather than the weight losses obtained at 2000°F (1093°C). Moreover, the weight gains of the single crystal alloys are significantly less than those for MAR M 200. Finally, the data for the single crystal alloys appear to follow a parabolic rate law. This may be the case for MAR M 200 also, but only up to about 1000 hours of testing. In Figure 7, the weight change versus time data for two of the single crystal alloys (Alloys A and C) are plotted to show conformance with the parabolic rate law. Some scatter in the data show that a small amount of cracking and spalling of the oxide scale has occurred. Nevertheless, it is apparent that these data can be approximated by a parabolic relationship. Similar results were obtained for the other single crystal alloys in the cyclic oxidation test at 1650°F (900°C). If the scatter in the measurements is not considered, the three single crystal alloys have parabolic rate constants of 1.5×10^{-15}, 0.9×10^{-14}, and 1.3×10^{-14} (g^2/cm^4-S) for Alloys A, B, and C, respectively. MAR M 200 conforms to the parabolic relationship for about 1000 hours and has a parabolic rate constant of 4.7×10^{-13} (g^2/cm^4-S). If data in the literature[5] for the growth of Al_2O_3 scales on Ni-Cr-Al alloys are used to obtain the parabolic rate constant for the growth of Al_2O_3 scales, a value of 1.10×10^{-14} (g^2/cm^4-S) is obtained. The results show that the oxidation kinetics for Alloys A, B, and C are controlled by the growth of Al_2O_3 scales. Parabolic growth may also be approached for the oxidation of MAR M 200 for exposure times of 1000 hours and less. These conclusions must be substantiated by metallographic observations since it is apparent that some cracking of the alumina scales is occurring during the thermal excursions, and is responsible for the very small parabolic rate constant of Alloy A.

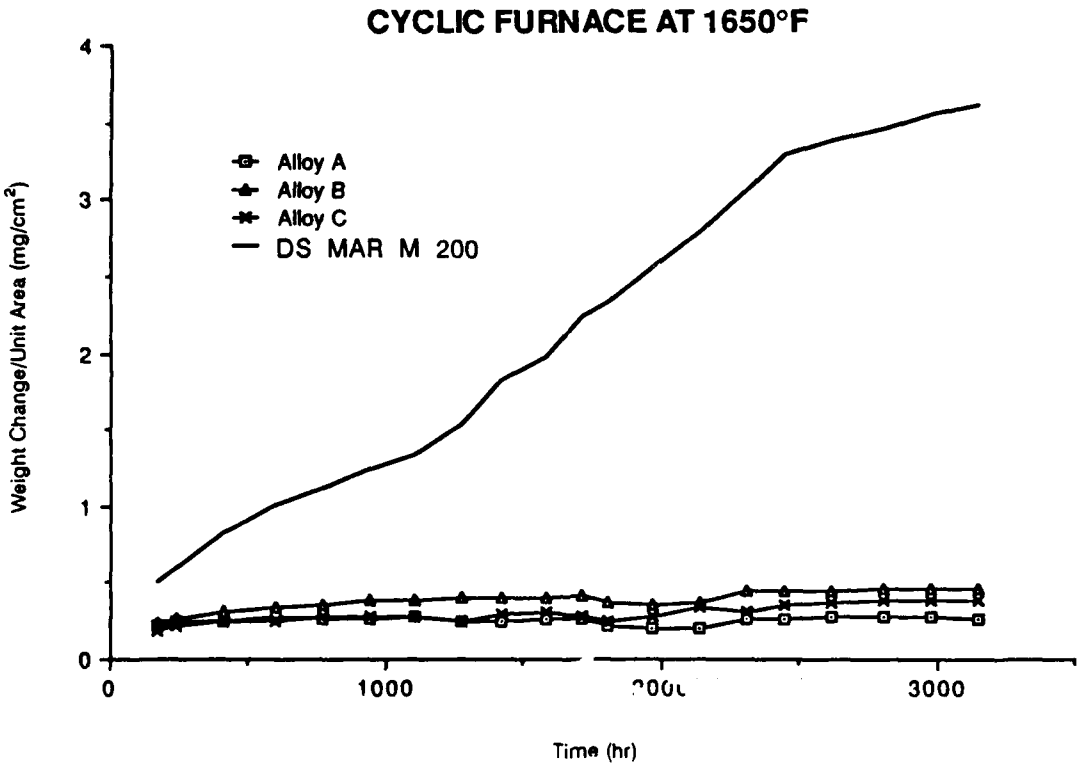

Figure 6. Weight change data for the cyclic oxidation of the alloys at 1650°F (900°C).

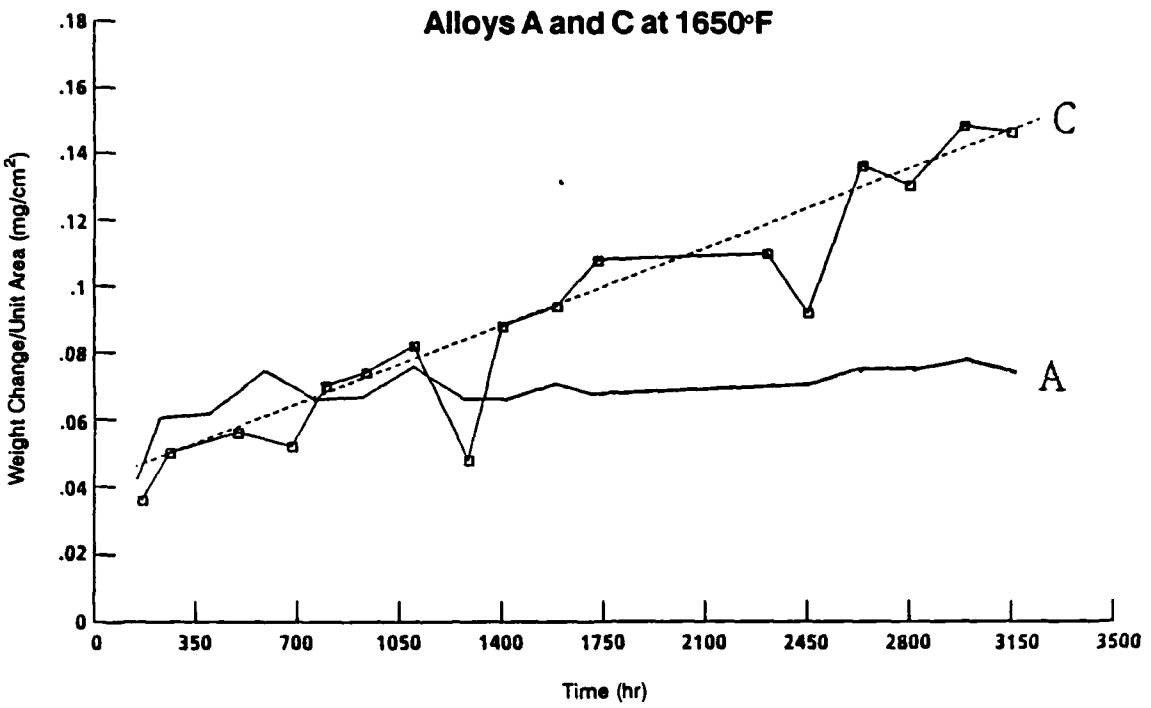

Figure 7. Weight change squared versus time data for Alloys A and C at 1650°F.

Figures 8 and 9 are typical degradation microstructures of MAR M 200 and one of the single crystal alloys after 3150 hours of exposure in the cyclic oxidation at 1650°F (900°C). The MAR M 200 specimen has a relatively thick external scale above the subscale Al_2O_3, as shown in Figure 8. Evidence of nitride formation is visible below this subscale zone in the zone which is denuded of γ'. Such microstructural features clearly show that this alloy is no longer an Al_2O_3 former. The microstructure typical of the single crystal alloys after exposure in the cyclic oxidation test at 1650°F (900°C) is presented in Figure 9. Zones of γ-phase adjacent to the surfaces of these alloys which are denuded of γ' have been formed. Moreover, zones of coarsened γ' are also evident beneath these γ zones. The coarsening of the γ' is being examined in more detail. Results available in the literature[6] indicate that this coarsening of γ' is due to recrystallization. Specimens of Alloy B were grit-blasted to create a surface totally covered with coarsened γ' upon recrystallization. The weight changes of such specimens during isothermal oxidation at 2000°F (1093°C) and 1650°F (900°C) were not different from those of specimens given the surface preparation described in the experimental section. The microstructure in Figure 9 is clearly consistent with external protective scales of Al_2O_3 having been present on the surfaces of these alloys during cyclic oxidation at 1650°F (900°C), since no internal oxidation is evident. The cyclic oxidation data obtained at 2000°F (1093°C) and 1650°F (900°C) show that the single crystal alloys have better oxidation resistance than MAR M 200. This is the same conclusion that was obtained from the tube furnace cyclic oxidation tests at 2000°F (1093°C) in a previous paper,[2] however, these data have now been corroborated by the burner rig tests at 2000°F (1093°C) and tube furnace cyclic oxidation testing at 1650°F (900°C). As discussed in a previous paper,[2] the better oxidation resistance of the single crystal alloys results from the different compositions of these alloys compared to MAR M 200, Table 1, rather than microstructural effects. The cyclic

6. OBLAK, J. M., and OWCZARSKI, W. A. *Cellular Recrystallization in a Nickel-Base Superalloy.* Trans. Met. Soc. of AIME. v. 242, 1968, p. 1563.

oxidation data obtained for the single crystal alloys at 1650°F (900°C) show that these alloys may not need coatings for applications at temperatures below about 1600°F (871°C).

Figure 8. Typical microstructural features developed on MAR M 200 after 3150 hours of cyclic oxidation at 1650°F (900°C).

Figure 9. Typical microstructural features developed on all of the single crystal superalloys after 3150 hours of cyclic oxidation at 1650°F (900°C).

The results from the burner rig tests and the tube furnace cyclic oxidation tests are essentially the same. The burner rig test is more severe and permits the differences in performance among the alloys to be discerned more quickly. It should be noted that the cycle used in the burner rig was such that more thermal cycling occurred in this test. On the other hand, the tube furnace is a much cheaper test and much more amenable to the controlled variation of critical parameters than the burner rig. The data obtained in the current investigation show that tube furnace cyclic oxidation can be used in place of burner rig oxidation tests. Longer times will be required to produce the degradation, but the temperature and gas composition can be maintained at controlled and defined levels throughout the test. Both of these tests must always be accompanied by detailed metallographic examination of the exposed specimens upon the conclusion of the test.

Cyclic Hot Corrosion

Weight change data for the Na_2SO_4-induced hot corrosion of the alloys at 1650°F (900°C) in air are presented in Figure 10. After about 100 hours, all of the alloys show large weight losses indicative of very severe hot corrosion attack. Typical degradation microstructures for MAR M 200 and one of the single crystal superalloys are presented in Figures 11 and 12. The microstructural features formed as a result of the hot corrosion of MAR M 200 and the single crystal alloys are the same. All of the alloys had thick corrosion products composed predominantly of oxides near the gas interface and of sulfides adjacent to the unaffected substrate. The hot corrosion behavior of all of the alloys in this test is comparable. The hot corrosion degradation microstructures are typical of those that are observed on structural alloys for high temperature Na_2SO_4-induced attack.[7,8]

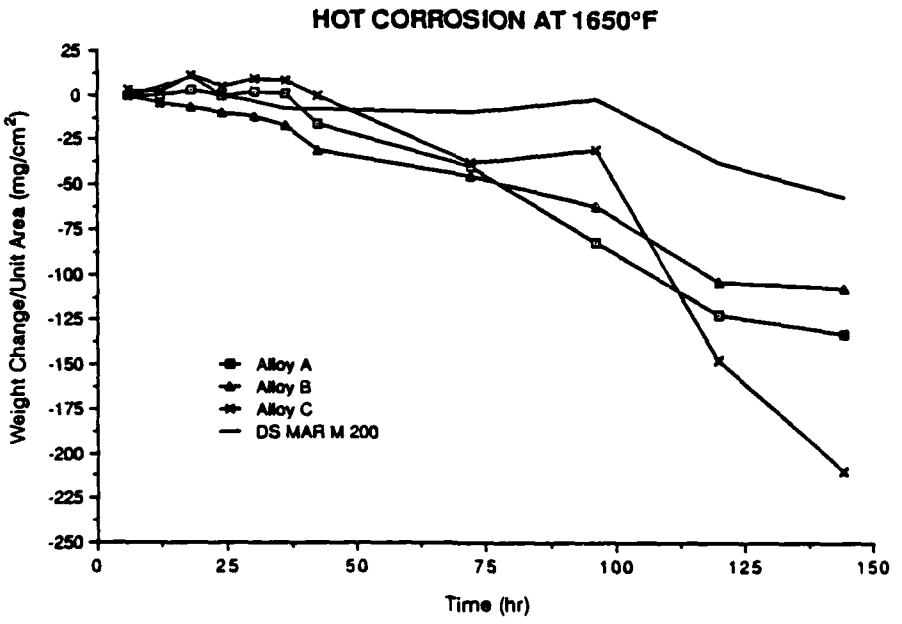

Figure 10. Weight change data for the Na_2SO_4-induced hot corrosion of the alloys at 1650°F (900°C) in air.

7. BORNSTEIN, N. S., and DECRESCENTE, M. A. Trans. Met. Soc. AIME, v. 245, 1969, p. 1947.
8. SEYBOLT, A. U. Trans. Met. Soc., v. 242, 1968, p. 1955.

Figure 11. Typical features observed after exposure of MAR M 200 in the cyclic hot corrosion test at 1650°F (1093°C).

When hot corrosion testing is performed at 1300°F (704°C), the gas composition is a more critical parameter than at 1650°F (900°C).[9] Furthermore, the composition of the salt deposit that is used is also important since some deposits may be solid. The initial hot corrosion tests at 1300°F (704°C) were performed using Na_2SO_4 deposits in air. After 100 hours of testing, all of the alloys exhibited a few milligrams/cm^2 of weight loss, which shows that the deposit was affecting the hot corrosion process. Based on the cyclic oxidation data obtained at 1650°F (900°C) for these alloys, very small weight gains would be expected for oxidation at 1300°F (704°C). A micrograph of a specimen exposed for 120 hours in this test is presented in Figure 13. The attack is small; nevertheless, there are some areas of localized degradation that show the deposit has affected the oxidation of all the alloys. In this test, it was not possible to determine if one of the alloys had been attacked less than the others.

In order to attempt to accelerate the hot corrosion attack at 1300°F (704°C), the tests were performed in air but using a Na_2SO_4 45-mole percent $MgSO_4$ deposit which is a liquid at 1300°F (704°C). The liquid deposit of Na_2SO_4 45-mole percent $MgSO_4$ caused much more severe attack of the alloys at 1300°F (704°C) than did Na_2SO_4. Weight change versus time data for this test is presented in Figure 14. The specimens were washed and brushed to remove loose corrosion products before weighing. Very substantial weight gains or losses for exposure at 1300°F (704°C) have been obtained (Figure 14). Even though some specimens gained weight and others lost weight, the magnitude of the weight changes are very large compared to those produced during oxidation. All of the alloys have undergone very severe hot corrosion degradation. In Figure 15, the microstructure of Alloy C is presented after 120 hours in the hot corrosion test using the Na_2SO_4 45-mole percent $MgSO_4$ composition. Some

9. BARKALOW, R. H., and PETTIT, F. S. *Proc. of the 4th Conference on Gas Turbine Materials in a Marine Environment.* Naval Sea Systems Command, Annapolis, MD, R., v. 493, 1979.

of the corrosion products have spalled from the surface of this specimen. Comparison of this microstructure to that presented in Figure 13 shows much more attack has occurred with the Na_2SO_4 45-mole percent $MgSO_4$ deposit. In Figures 16 and 17, the microstructures of MAR M 200 and one of the single crystal alloys are presented upon termination of the cyclic hot corrosion tests using deposits of Na_2SO_4 45-mole percent $MgSO_4$ after 750 hours. The amount of attack is extremely severe for all of the alloys, but a ranking is not possible. Tungsten and tantalum were detected in the corrosion products by energy dispersive analysis. It is not the purpose of this report to attempt to develop models for the hot corrosion of these alloys. A liquid deposit produces more attack of these alloys. Based upon data available in the literature,[8] the hot corrosion of these alloys should be affected by their refractory metal content. Therefore, it is proposed that the rapid hot corrosion is caused by the liquid deposit reacting with oxides of the refractory elements in these alloys.

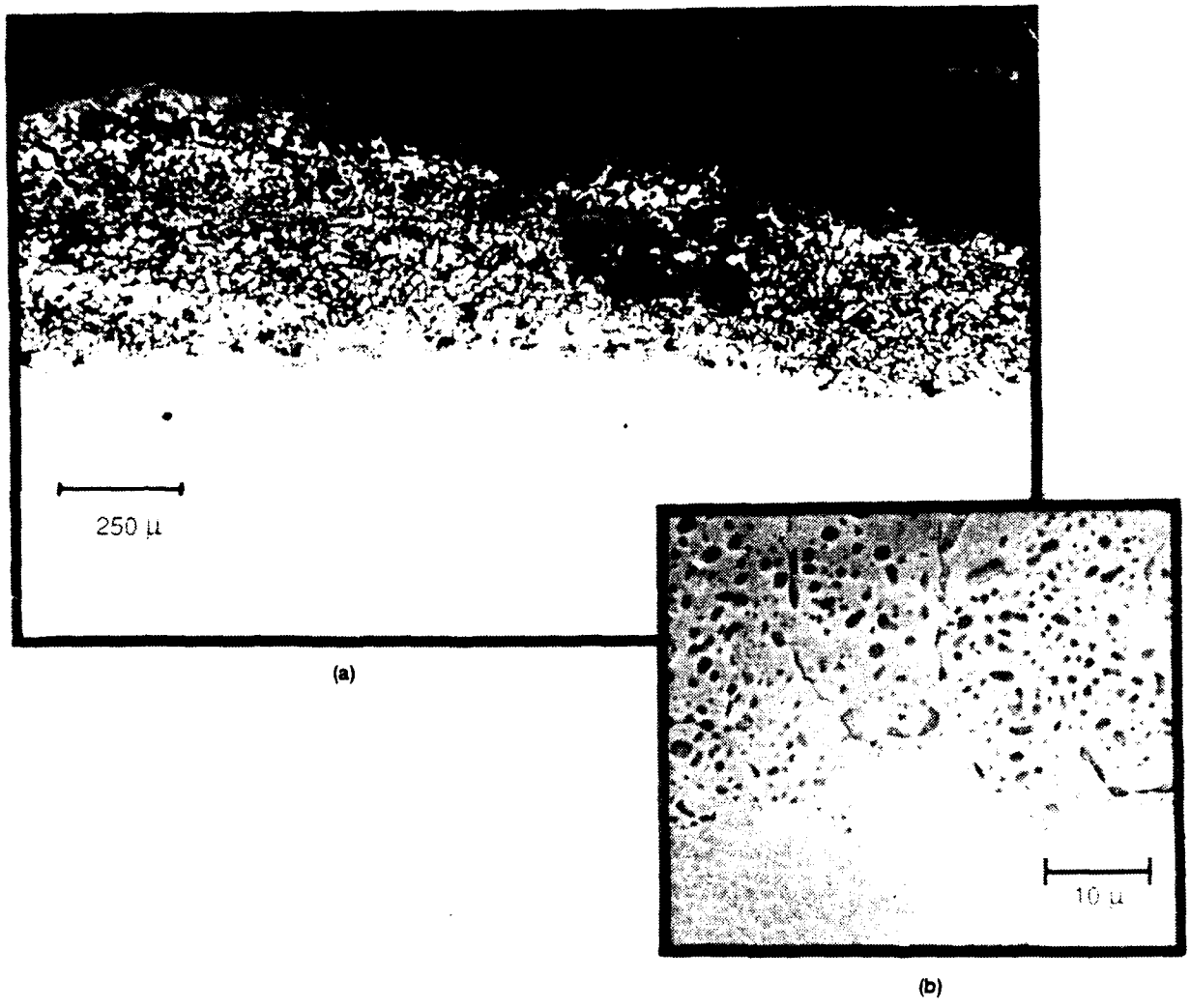

Figure 12. Typical features observed after exposure of the single crystal alloys in the cyclic hot corrosion test at 1650°F (1093°C), (a) corrosion products, (b) sulfides at corrosion products - alloy interface.

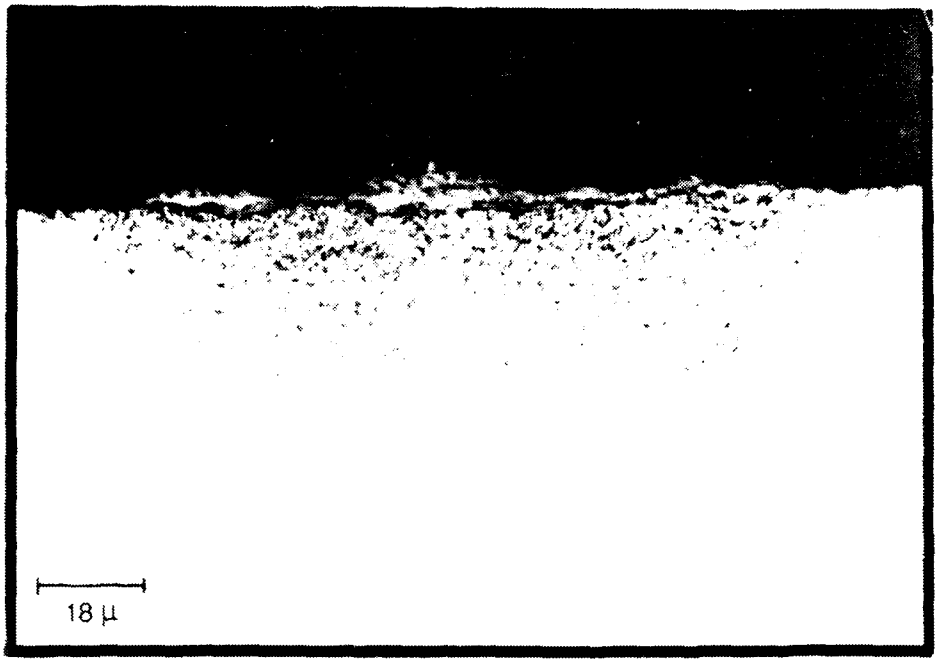

Figure 13. Typical microstructural features that developed on MAR M 200 and on the single crystal alloys after 120 hours of cyclic hot corrosion at 1300°F (704°C) using deposits of Na_2SO_4 (Alloy B).

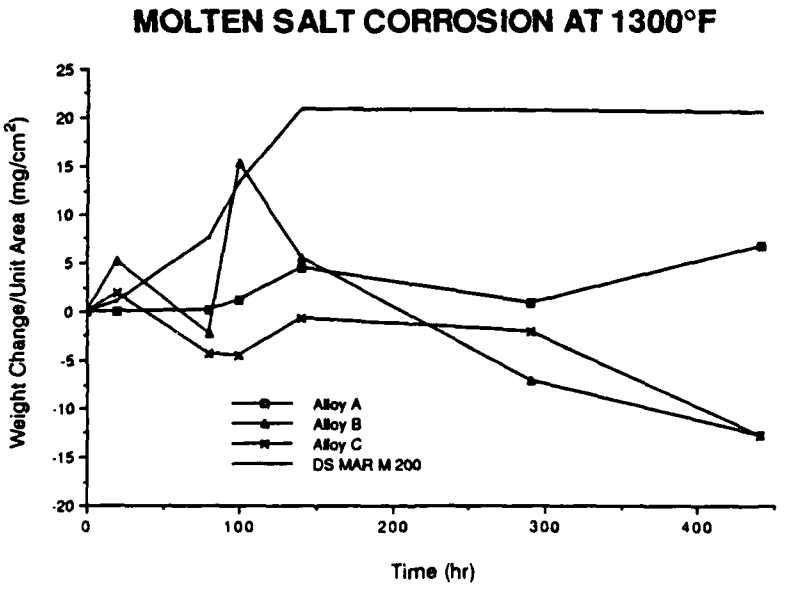

Figure 14. Weight change data versus time data for the cyclic hot corrosion of all the alloys at 1300°F (704°C) in air using deposits of Na_2SO_4 45-mole percent $MgSO_4$.

Figure 15. Photomicrograph of Alloy C after 120 hours in the cyclic hot corrosion test at 1300°F (704°C) using Na_2SO_4 45-mole percent $MgSO_4$ deposit.

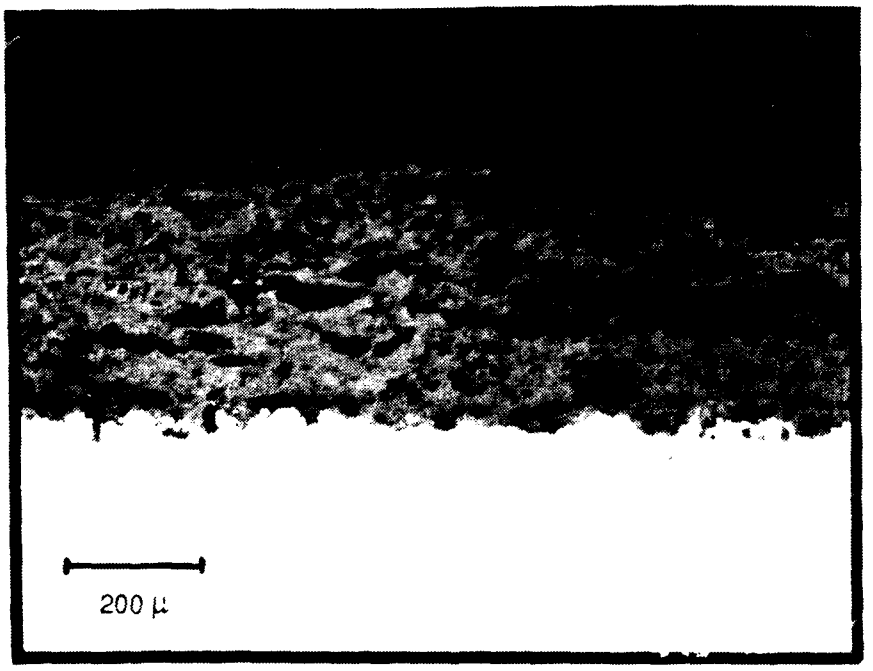

Figure 16. Photomicrograph showing microstructures of MAR M 200 upon conclusion of the cyclic hot corrosion test (750 hours) at 1300°F (704°C) using deposits of Na_2SO_4 45-mole percent MgSO4.

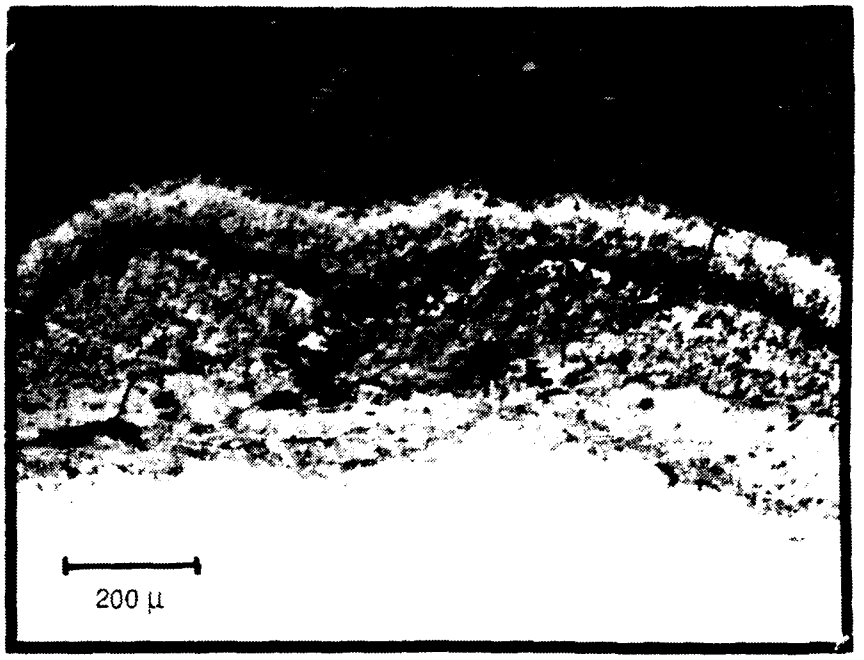

Figure 17. Photomicrograph showing microstructures of Alloy A upon conclusion of the cyclic hot corrosion test (750 hours) at 1300°F (704°C) using deposits of Na_2SO_4 45-mole percent MgSO4.

At 1300°F (704°C), the hot corrosion of many alloys becomes more severe as SO_3 is added to gas mixtures containing oxygen. Such a test is not really critical to the hot corrosion of the alloys studied in this program because very severe attack of all of the alloys occurred in air. Nevertheless, in order to provide a comparison, one of the single crystal alloys was coated with deposits of Na_2SO_4 45-mole percent $MgSO_4$ and exposed isothermally at 1300°F (704°C) to oxygen containing SO_3 at 3×10^{-5} atm. The weight change as a function of time for one of these specimens is presented in Figure 18. The weight change data show that very significant attack is occurring since virtually no weight change would be observed for this alloy in the absence of the deposit at this temperature. A photomicrograph of the specimen exposed to the conditions described in Figure 18 is presented in Figure 19. Very substantial attack is evident after an exposure time of 24 hours. A specimen of the alloy that was used in the experiment with Na_2SO_4 45-mole percent $MgSO_4$ deposit and exposed at 700°F in oxygen with SO_3 was also exposed under the same conditions but with no deposit on its surface. The resulting weight change after 20 hours is indicated in Figure 18. This weight change is very small. The absence of attack was also confirmed by visual examination of the specimen upon conclusion of this test. These results shown that the liquid deposit is the most important parameter in causing the hot corrosion attack of the alloys rather than the composition of the gas. The attack may be more severe when SO_3 is present in the gas, but also occurs at an unacceptably high rate in air. In the case of hot corrosion resistant coatings, the composition of the gas is critical, and SO_3 is required for attack to occur. In the case of nickel-base superalloys, however, the presence of refractory metal oxides must be a sufficient condition to cause severe hot corrosion attack even in the absence of SO_3.

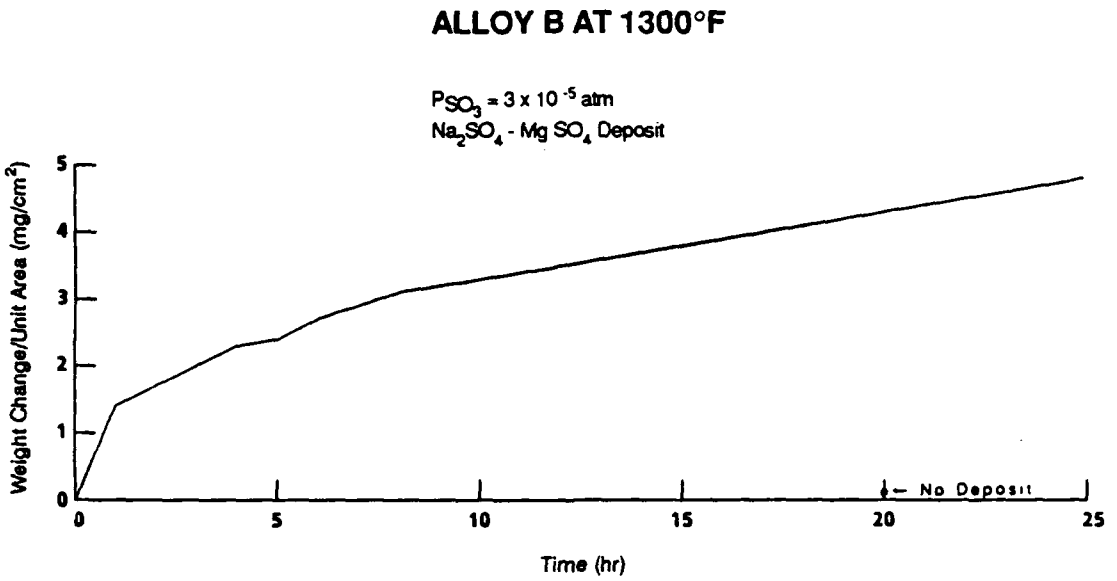

Figure 18. Weight change versus time data for the isothermal hot corrosion (Na_2SO_4 45-mole percent $MgSO_4$ deposit) of a single crystal alloy (Alloy B) at 1300°F (704°C) in oxygen with an SO_3 pressure of 3 x 10^{-5} atm. Data are also presented for the alloy exposed to the same conditions but with no deposits on its surface.

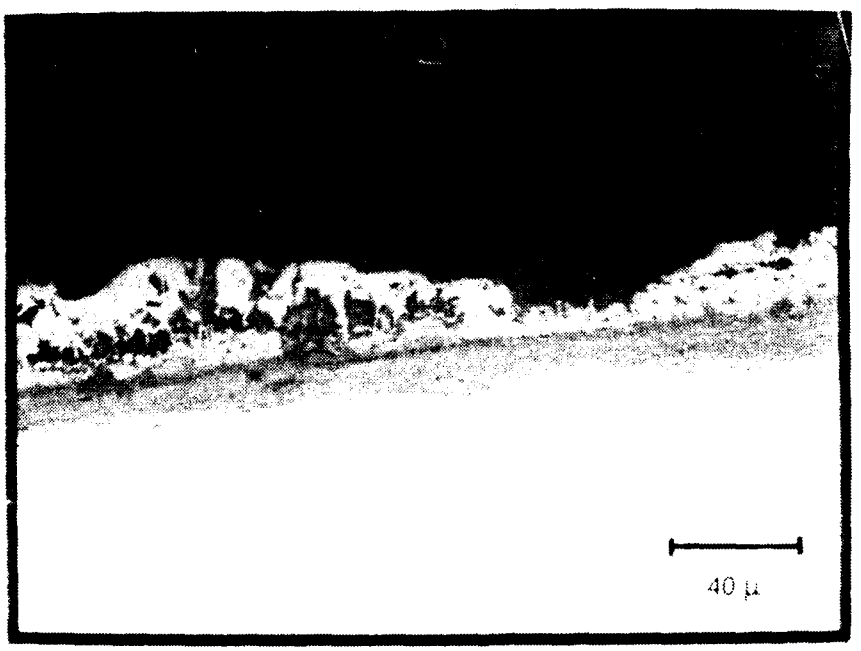

Figure 19. Typical photomicrograph of single crystal alloy after exposure to hot corrosion conditions at 1300°F (704°C) with oxygen-containing SO_3 at a pressure of 3 x 10^{-5} atm.

CONCLUSIONS

Nickel-base alloys have been tested at 2000°F (1093°C) in cyclic oxidation tests using a tube furnace and a burner rig. The same ranking of the alloys was obtained in both tests with the single crystal superalloys having better oxidation resistance than the directionally solidified alloy MAR M 200. These results show that tube furnace tests can be used in place of burner rig tests to rank alloys providing that the tests are accompanied with detailed metallographic examination of the exposed specimens. This ensures that the conditions produce degradational microstructures similar to those of the burner rig or the service application of interest.

Oxidation tests at 1650°F (900°C) using the tube furnace produced a ranking of the alloys consistent with the 2000°F (1093°C) results and showed that the nickel-base single crystal alloys had protective scales of Al_2O_3 that did not extensively crack or spall after 3000 hours of cyclic oxidation. The single crystal alloys probably can be used uncoated for applications involving oxidizing conditions and temperatures below 1650°F (900°C).

All of the alloys were severely degraded when a liquid sulfate deposit was placed upon their surfaces at 1650°F (900°C) and 1300°F (704°C). There is no significant difference between the hot corrosion resistance of these alloys when tested in air or in oxygen with SO_3, provided a liquid deposit was present in both cases. All of the alloys would require a coating if they were to be exposed to any type of hot corrosion conditions at temperatures of 1300°F (704°C) or higher.

DISTRIBUTION LIST

No. of Copies	To
1	Office of the Under Secretary of Defense for Research and Engineering, The Pentagon, Washington, DC 20301
	Commander, U.S. Army Laboratory Command, 2800 Powder Mill Road, Adelphi, MD 20783-1145
1	ATTN: AMSLC-IM-TL
	Commander, Defense Technical Information Center, Cameron Station, Building 5, 5010 Duke Street, Alexandria, VA 22304-6145
2	ATTN: DTIC-FDAC
	Metals and Ceramics Information Center, Battelle Columbus Laboratories, 505 King Avenue, Columbus, OH 43201
1	ATTN: Harold Mindlin
	Commander, Army Research Office, P.O. Box 12211, Research Triangle Park, NC 27709-2211
1	ATTN: Information Processing Office
	Commander, U.S. Army Materiel Command (AMC), 5001 Eisenhower Avenue, Alexandria, VA 22333
1	ATTN: AMCLD
1	AMCPO-BD
	Commander, U.S. Army Materiel Systems Analysis Activity, Aberdeen Proving Ground, MD 21005
1	ATTN: AMXSY-MP, Director
	Commander, U.S. Army Missile Command, Redstone Scientific Information Center, Redstone Arsenal, AL 35898-5241
1	ATTN: AMSMI-RD-CS-R/Doc
1	AMSMI-CS, R. B. Clem
1	AMSMI-RD-ST-CM
	Commander, U.S. Army Armament, Munitions and Chemical Command, Dover, NJ 07801
2	ATTN: Technical Library
	Commander, U.S. Army Tank-Automotive Command, Warren, MI 48397-5000
1	ATTN: AMSTA-ZSK
2	AMSTA-TSL, Technical Library
1	AMSTA-RCK
	Commander, U.S. Army Foreign Science and Technology Center, 220 7th Street, N.E., Charlottesville, VA 22901
1	ATTN: Military Tech
	Director, Eustis Directorate, U.S. Army Air Mobility Research and Development Laboratory, Fort Eustis, VA 23604
1	ATTN: SAVDL-E-MOS (AVSCOM)
1	SAVDL-EU-TAP
	U.S. Army Aviation Training Library, Fort Rucker, AL 36360
1	ATTN: Building 5906--5907
	Commander, U.S. Army Aviation Systems Command, 4300 Goodfellow Boulevard, St. Louis, MO 63166
1	ATTN: AMDAV-EGX
1	AMDAV-EX, Mr. R. Lewis
1	AMDAV-EQ, Mr. Crawford
2	AMCPM-AAH-TM, Mr. R. Hubbard, Mr. B. J. Baskett
1	AMDAV-DS, Mr. W. McClane
	Naval Research Laboratory, Washington, DC 20375
1	ATTN: Code 5830
1	Code 2627

No. of Copies	To
	Chief of Naval Research, Arlington, VA 22217
1	ATTN: Code 471
	Director, Structural Mechanics Research, Office of Naval Research, 800 North Quincy Street, Arlington, VA 22203
1	ATTN: Dr. M. Perrone
1	Edward J. Morrissey, AFWAL/MLTE, Wright Patterson Air Force Base, OH 45433
	Commander, U.S. Air Force Wright Aeronautical Laboratories, Wright-Patterson Air Force Base, OH 45433
1	ATTN: AFWAL/MLC
1	AFWAL/MLLP, D. M. Forney, Jr.
1	AFWAL/MLBC, Mr. Stanley Schulman
1	AFWAL/MLXE, A. Olevitch
	National Aeronautics and Space Administration, Marshall Space Flight Center, Huntsville, AL 35812
1	ATTN: R. J. Schwinghammer, EH01, Dir, M&P Lab
1	Mr. W. A. Wilson, EH41, Bldg. 4612
	Chief of Naval Research, Washington, DC 20350
1	ATTN: OP-987, Director
	Aeronautical Systems Division (AFSC), Wright-Patterson Air Force Base, OH 45433
1	ATTN: ASD/ENFEF, D. C. Wight
1	ASD/ENFTV, D. J. Wallick
1	ASD/XRHD, G. B. Bennett
	Air Force Armament Laboratory, Eglin Air Force Base, FL 32542
1	ATTN: AFATL/DLYA, V. D. Thornton
	Air Force Flight Dynamics Laboratory, Wright-Patterson Air Force Base, OH 45433
1	ATTN: AFFDL/FIES, J. Sparks
1	AFFDL/FIES, J. Hodges
1	AFFDL/TST, Library
	Air Force Test and Evaluation Center, Kirtland Air Force Base, NM 87115
1	ATTN: AFTEC-JT
	NASA - Ames Research Center, Army Air Mobility Research and Development Laboratory, Mail Stop 207-5, Moffett Field, CA 94035
1	ATTN: SAVDL-AS-X, F. H. Immen
	NASA - Johnson Spacecraft Center, Houston, TX 77058
1	ATTN: JM6
1	ES-5
	Naval Air Development Center, Warminster, PA 18974
1	ATTN: Code 063
1	Code 6062
	Naval Air System Command, Department of the Navy, Washington, DC 20360
1	ATTN: AIR-03PAF
1	AIR-5203
1	AIR-5164J
1	AIR-530313
	Naval Post Graduate School, Monterey, CA 93948
1	ATTN: Code 578P, R. E. Ball
	Naval Surface Weapons Center, Dahlgren Laboratory, Dahlgren, VA 22448
1	ATTN: Code G-54, Mr. J. Hall
1	Code G-54, Dr. B. Smith

No. of Copies	To
	Commander, Rock Island Arsenal, Rock Island, IL 61299
1	ATTN: AMSAR-PPV
	Armament Systems, Inc., 712-F North Valley, Anaheim, CA 92801
1	ATTN: J. Musch
	Beech Aircraft Corporation, 9709 E. Central Avenue, Wichita, KS 67206
1	ATTN: Engineering Library
	Bell Helicopter Company, A Textron Company, P.O. Box 482, Fort Worth, TX 76101
1	ATTN: J. R. Johnson
	Boeing Helicopters, P.O. Box 16858, Philadelphia, PA 19142-0858
1	ATTN: N. Caravasos M/S P30-27
1	Cessna Military, P.O. Box 7704, Wichita, KS 67277-7704
	Fairchild Industries, Inc., Fairchild Republic Company, Conklin Street, Farmingdale, Long Island, NY 11735
1	ATTN: Engineering Library, G. A. Mauter
	FMC Corporation, Central Engineering Labs, 1185 Coleman Avenue, Box 80, Santa Clara, CA 95052
1	ATTN: Gary L. Boerman
	FMC Corporation, Ordnance Division, 1105 Coleman Avenue, Box 1201, San Jose, CA 95108
1	ATTN: William H. Altergott
	General Dynamics Corporation, Convair Division, P.O. Box 80877, San Diego, CA 92138
1	ATTN: Research Library, U. J. Sweeney
	Gruman Aerospace Corporation, South Oyster Bay Road, Bethpage, NY 11714
1	ATTN: Technical Information Center, J. Davis
	McDonnell Douglas Helicopter Co., 5000 East McDowell Road, Mesa, AZ 85205-9797
1	ATTN: Library
	IIT Research Institute, 10 West 35th Street, Chicago, IL 60616
1	ATTN: K. McKee
	Kaman Aerospace Corporation, Old Winsor Road, Bloomfield, CT 06002
1	ATTN: H. E. Showalter
	Lockheed-California Company, A Division of Lockheed Aircraft Corporation, Burbank, CA 91503
1	ATTN: Technological Information Center, 84-40, U-35, A-1
	Vought Corporation, P.O. Box 5907, Dallas, TX 75232
1	ATTN: D. M. Reedy, 2-30110
	Martin Marietta Corporation, Orlando Division, P.O. Box 5837, Orlando, Fl 32805
1	ATTN: Library, M. C. Griffith
	McDonnell Douglas Corporation, 3855 Lakewood Boulevard, Long Beach, CA 90846
1	ATTN: Technical Library, Cl 290/36-84
	Northrop Corporation, Aircraft Division, 3901 W. Broadway, Hawthorne, CA 90250
1	ATTN: Mgr. Library Services, H. W. Jones
	Parker Hannifin, 14300 Alton Pkwy., Irvine, CA 92718-1814
1	ATTN: C. Beneker

No. of Copies	To
	Sikorsky Aircraft, A Division of United Aircraft Corporation, Main Street, Stratford, CT 06601
1	ATTN: Mel Schwartz, Chief of Metals
	Teledyne CAE, 1330 Laskey Road, Toledo, OH 43697
1	ATTN: Librarian
	Georgia Institute of Technology, School of Mechanical Engineering, Atlanta, GA 30332
1	ATTN: Mechanical Engineering Library
	Lukens Steel Company, Coateville, PA 19320
1	ATTN: Dr. E. Hamburg
1	Mr. A. Wilson
	Republic Steel Corporation, 410 Oberlin Avenue SW, Massillon, OH 44646
1	ATTN: Mr. R. Sweeney
1	Mr. W. H. Brechtel
1	Mr. T. M. Costello
	L. Raymond Associates, P.O. Box 7925, Newport Beach CA 92658-7925
1	ATTN: Dr. L. Raymond
	Ingersoll Rand Oilfield Products Division, P.O. Box 1101, Pampa, TX 79065
1	ATTN: Mr. W. L. Hallerberg
	Brown University, Division of Engineering, Providence, RI 02912
1	ATTN: Prof. J. Duffy
	SRI International, 333 Ravenswood Avenue, Menlo Park, CA 94025
1	ATTN: Dr. D. Shockey
	Illinois Institute of Technology, Metallurgical and Materials Engineering Department, Chicago, IL 60616
1	ATTN: Dr. Norman Breyer
	Corpus, Christi Army Depot, Corpus Christi, TX 78419
1	ATTN: SDSCC-QLS
	U.S. Army Materials Technology Laboratory, Watertown, MA 02172-0001
2	ATTN: SLCMT-TML
3	Authors

U.S. Army Materials Technology Laboratory
Watertown, Massachusetts 02172-0001
OXIDATION AND HOT CORROSION OF SOME ADVANCED SUPERALLOYS AT 1300°F TO 2000°F (704°C TO 1093°C) -
Milton Levy, Robert M. Huie, and Fred Pettit

AD________________
UNCLASSIFIED
UNLIMITED DISTRIBUTION

Technical Report MTL TR 89-26, April 1989, 20 pp-illus-table, D/A Project: 1L162105.AH84

Key Words

Superalloys
Nickel-base superalloys
Oxidation resistance

The cyclic oxidation resistance and the hot corrosion resistance of three single crystal nickel-base superalloys and DS MAR M 200 are compared. The comparison is made by using burner rig oxidation tests at 2000°F (1093°C), and tube furnace oxidation and hot corrosion tests at 2000°F (1093°C), 1650°F (900°C), and 1300°F (704°C). The rig tests and the tube furnace tests produce similar results with the single crystal alloys being more oxidation resistant than DS MAR M 200. A significant difference between the hot corrosion resistance of these alloys was not observed. All four alloys were extremely susceptible to hot corrosion induced by a liquid deposit.

U.S. Army Materials Technology Laboratory
Watertown, Massachusetts 02172-0001
OXIDATION AND HOT CORROSION OF SOME ADVANCED SUPERALLOYS AT 1300°F TO 2000°F (704°C TO 1093°C) -
Milton Levy, Robert M. Huie, and Fred Pettit

AD________________
UNCLASSIFIED
UNLIMITED DISTRIBUTION

Technical Report MTL TR 89-26, April 1989, 20 pp-illus-table, D/A Project: 1L162105.AH84

Key Words

Superalloys
Nickel-base superalloys
Oxidation resistance

The cyclic oxidation resistance and the hot corrosion resistance of three single crystal nickel-base superalloys and DS MAR M 200 are compared. The comparison is made by using burner rig oxidation tests at 2000°F (1093°C), and tube furnace oxidation and hot corrosion tests at 2000°F (1093°C), 1650°F (900°C), and 1300°F (704°C). The rig tests and the tube furnace tests produce similar results with the single crystal alloys being more oxidation resistant than DS MAR M 200. A significant difference between the hot corrosion resistance of these alloys was not observed. All four alloys were extremely susceptible to hot corrosion induced by a liquid deposit.

U.S. Army Materials Technology Laboratory
Watertown, Massachusetts 02172-0001
OXIDATION AND HOT CORROSION OF SOME ADVANCED SUPERALLOYS AT 1300°F TO 2000°F (704°C TO 1093°C) -
Milton Levy, Robert M. Huie, and Fred Pettit

AD________________
UNCLASSIFIED
UNLIMITED DISTRIBUTION

Technical Report MTL TR 89-26, April 1989, 20 pp-illus-table, D/A Project: 1L162105.AH84

Key Words

Superalloys
Nickel-base superalloys
Oxidation resistance

The cyclic oxidation resistance and the hot corrosion resistance of three single crystal nickel-base superalloys and DS MAR M 200 are compared. The comparison is made by using burner rig oxidation tests at 2000°F (1093°C), and tube furnace oxidation and hot corrosion tests at 2000°F (1093°C), 1650°F (900°C), and 1300°F (704°C). The rig tests and the tube furnace tests produce similar results with the single crystal alloys being more oxidation resistant than DS MAR M 200. A significant difference between the hot corrosion resistance of these alloys was not observed. All four alloys were extremely susceptible to hot corrosion induced by a liquid deposit.

U.S. Army Materials Technology Laboratory
Watertown, Massachusetts 02172-0001
OXIDATION AND HOT CORROSION OF SOME ADVANCED SUPERALLOYS AT 1300°F TO 2000°F (704°C TO 1093°C) -
Milton Levy, Robert M. Huie, and Fred Pettit

AD________________
UNCLASSIFIED
UNLIMITED DISTRIBUTION

Technical Report MTL TR 89-26, April 1989, 20 pp-illus-table, D/A Project: 1L162105.AH84

Key Words

Superalloys
Nickel-base superalloys
Oxidation resistance

The cyclic oxidation resistance and the hot corrosion resistance of three single crystal nickel-base superalloys and DS MAR M 200 are compared. The comparison is made by using burner rig oxidation tests at 2000°F (1093°C), and tube furnace oxidation and hot corrosion tests at 2000°F (1093°C), 1650°F (900°C), and 1300°F (704°C). The rig tests and the tube furnace tests produce similar results with the single crystal alloys being more oxidation resistant than DS MAR M 200. A significant difference between the hot corrosion resistance of these alloys was not observed. All four alloys were extremely susceptible to hot corrosion induced by a liquid deposit.